MIT Joint Program on the Science and Policy of Global Change

Assessing Evapotranspiration Estimates from the Global Soil Wetness Project Phase 2 (GSWP-2) Simulations

C. Adam Schlosser and Xiang Gao

Report No. 179
September 2009

The MIT Joint Program on the Science and Policy of Global Change is an organization for research, independent policy analysis, and public education in global environmental change. It seeks to provide leadership in understanding scientific, economic, and ecological aspects of this difficult issue, and combining them into policy assessments that serve the needs of ongoing national and international discussions. To this end, the Program brings together an interdisciplinary group from two established research centers at MIT: the Center for Global Change Science (CGCS) and the Center for Energy and Environmental Policy Research (CEEPR). These two centers bridge many key areas of the needed intellectual work, and additional essential areas are covered by other MIT departments, by collaboration with the Ecosystems Center of the Marine Biology Laboratory (MBL) at Woods Hole, and by short- and long-term visitors to the Program. The Program involves sponsorship and active participation by industry, government, and non-profit organizations.

To inform processes of policy development and implementation, climate change research needs to focus on improving the prediction of those variables that are most relevant to economic, social, and environmental effects. In turn, the greenhouse gas and atmospheric aerosol assumptions underlying climate analysis need to be related to the economic, technological, and political forces that drive emissions, and to the results of international agreements and mitigation. Further, assessments of possible societal and ecosystem impacts, and analysis of mitigation strategies, need to be based on realistic evaluation of the uncertainties of climate science.

This report is one of a series intended to communicate research results and improve public understanding of climate issues, thereby contributing to informed debate about the climate issue, the uncertainties, and the economic and social implications of policy alternatives. Titles in the Report Series to date are listed on the inside back cover.

Henry D. Jacoby and Ronald G. Prinn,
Program Co-Directors

For more information, please contact the Joint Program Office

Postal Address: Joint Program on the Science and Policy of Global Change
77 Massachusetts Avenue
MIT E19-411
Cambridge MA 02139-4307 (USA)

Location: 400 Main Street, Cambridge
Building E19, Room 411
Massachusetts Institute of Technology

Access: Phone: +1(617) 253-7492
Fax: +1(617) 253-9845
E-mail: globalchange@mit.edu
Web site: http://globalchange.mit.edu/

Printed on recycled paper

Assessing Evapotranspiration Estimates from the Global Soil Wetness Project Phase 2 (GSWP-2) Simulations

C. Adam Schlosser* and Xiang Gao

Abstract

We assess the simulations of global-scale evapotranspiration from the Global Soil Wetness Project Phase 2 (GSWP-2) within a global water-budget framework. The scatter in the GSWP-2 global evapotranspiration estimates from various land surface models can constrain the global, annual water budget fluxes to within ±2.5%, and by using estimates of global precipitation, the residual ocean evaporation estimate falls within the range of other independently derived bulk estimates. However, the GSWP-2 scatter cannot entirely explain the imbalance of the annual fluxes from a modern-era, observationally-based global water budget assessment, and inconsistencies in the magnitude and timing of seasonal variations between the global water budget terms are found. Inter-model inconsistencies in evapotranspiration are largest for high latitude inter-annual variability as well as for inter-seasonal variations in the tropics, and analyses with field-scale data also highlights model disparity at estimating evapotranspiration in high latitude regions. Analyses of the sensitivity simulations that replace uncertain forcings (i.e. radiation, precipitation, and meteorological variables) indicate that global (land) evapotranspiration is slightly more sensitive to precipitation than net radiation perturbations, and the majority of the GSWP-2 models, at a global scale, fall in a marginally moisture-limited evaporative condition. Finally, the range of global evapotranspiration estimates among the models is larger than any bias caused by uncertainties in the GSWP-2 atmospheric forcing, indicating that model structure plays a more important role toward improving global land evaporation estimates (as opposed to improved atmospheric forcing).

Contents

1. INTRODUCTION

In the quest to accurately portray global hydro-climate conditions as well as predict variations, potential changes, and impacts of the climate system, evapotranspiration is regarded as one of the critical fluxes that links the energy, water, and biogeochemical cycles of the terrestrial eco-hydrological systems. However, with respect to our ability of direct measurement, evapotranspiration is a key, missing variable in global water-balance assessments (Swenson and

* MIT Joint Program on the Science and Policy of Global Change, Cambridge, MA 02139
Email: casch@mit.edu

Wahr, 2006) as well as for regional assessments of hydro-climatologic variability and change (Werth and Avissar, 2004). At large spatial scales for climate studies, it is an inherently difficult flux to measure directly, and a variety of other methods have been aimed to estimate and assess its mean state and variability. More recent observationally based residual estimates of evapotranspiration have been provided at basin (Rodell *et al.,* 2004a) to continental scales (Karam and Bras, 2008 and Walter *et al*., 2004), and show promise in the ability of these methods to estimate mean fluxes as well as their variability and possible trends. Other techniques for evapotranspiration estimation using remotely sensed data (Wang *et al.*, 2007 and Song *et al.*, 2000) have been undergoing refinement and have been provisionally analyzed at a global scale (Wang and Liang, 2008). However, data availability and sensitivity to retrieval and interpolation errors (in temperature and vegetation properties) continue to be significant issues with these sorts of techniques. As such, reliable and comprehensive direct and/or derived measurements of global or large-scale evapotranspiration remain elusive.

In light of this, the climate-research community has placed a heavy reliance upon modeling and assimilation techniques to estimate land evapotranspiration (as well as other land flux and state variables). Many such models are actively in use within the climate-research community (Rodell *et al.*, 2004b) and represent a variety of parameterization recipes to represent key biogeophysical and biogeochemical processes. Evaluation of these model simulations, wherever possible, is of considerable interest in order to document their reliability and consistency. Further, with the multiple model-based estimates comes a degree of uncertainty that must also be quantified, and done so preferably within the context of complementary, and wherever possible, directly comparable measurements of other water cycle storages and fluxes.

In previous studies, direct comparisons of models used to estimate evapotranspiration have proven quite useful in this regard (Chen *et al*., 1997; Werth and Avissar, 2004; and Su *et al.*, 2005), yet most of these analyses were of limited spatial and/or temporal coverage. Recently, the Global Soil Wetness Project Phase 2 (GSWP-2, IGPO 2002) has provided an unprecedented collection of global simulations spanning the 1986-1995 period of land states and fluxes calculated from 13 participating biogeophysical models used in climate research and weather prediction. The simulations provide a baseline set of runs as well as additional subsets of sensitivity runs that consider sources of uncertainty in the required atmospheric inputs and land cover fields. The GSWP-2 simulation period also falls within the time domain of a recent modern-era assessment of the global water cycle (Schlosser and Houser, 2007 – hereafter referred to as SH07), in which an absence of uncertainty estimates for global land evapotranspiration was highlighted. In view of these issues, we have analyzed the outputs of evapotranspiration from the GSWP-2 model simulations to serve a few key purposes: 1) to provide global estimates of land evapotranspiration rates to complement a modern-era, observationally based global water cycle assessment; 2) to quantify the uncertainty in these evapotranspiration estimates and; 3) determine the primary sources of these uncertainties (i.e. from models or inputs) as well as areas where evapotranspiration estimates are in most need for improvement. In the section that follows, we describe the GSWP-2 model experiments that include outputs of a baseline and sensitivity runs used for this study. In addition, we also describe the data taken from a global water budget assessment employed for our analysis as well as field data used for a complementary evaluation of the GSWP-2 simulations. Section 3 describes the results of our analysis, and finally, in section 4 we present our conclusions and closing remarks for continued research.

2. DATA

2.1 Global Soil Wetness Project Phase 2 (GSWP-2)

The Global Soil Wetness project (GSWP) is an element of the Global Land-Atmosphere System Study (GLASS) and a study of the GEWEX Modeling and Prediction Panel (GMPP), both contributing projects of the Global Energy and Water Cycle Experiment (GEWEX). GSWP is charged with producing large-scale data sets of soil moisture, temperature, runoff, and surface fluxes by integrating one-way offline land surface schemes (LSSs) using externally specified surface forcing and standardized soil and vegetation distributions. The GSWP-2 (see Dirmeyer *et al*., 2006 for details) produced a 10-year daily global gridded data set of land surface state variables and fluxes - excluding Antarctica. To gauge the impact of this omission in this global-scale modeling effort, we have also obtained an estimate of annual evaporation over Antarctica using the technique described by Loewe (1957). GSWP-2 is closely linked to the ISLSCP Initiative II data effort (Hall *et al*., 2006), and the LSSs simulations in GSWP-2 encompass the same 10-year core period (1986 – 1995). The model simulations are conducted on a 1°x 1° grid, and each model is driven by identical meteorological forcings. The 3-hourly near-surface meteorological forcing data sets are derived from the regridding of the National Centers for Environmental Prediction (NCEP)/Department of Energy (DOE) reanalyses (Kanamitsu *et al*., 2002), with corrections to the systematic biases in the reanalysis fields made by hybridization with global observationally-based gridded data sets (Zhao and Dirmeyer, 2003). This provides the land models with some of the most accurate forcing data available.

Thirteen LSSs in use today within the climate modeling community have participated in the baseline (B0) simulation for GSWP-2 (**Table 1**), and constitute a broad cross-section of numerical recipes to parameterize biogeophysical land processes. All the participating models adhere to the same land mask, and as closely as possible to the supplied data sets of vegetation distribution and properties, soil properties, surface albedos, etc. They also follow the same procedure for spin-up process with the same initial condition (soil temperature, soil moisture, and snow cover) and report a standard set of output data for the 10-year core period 1986-1995. The results from the land surface models were checked for quality, consistency and conservation of mass and energy, corrected when problems were detected, and then combined to produce a multi-model land-surface analysis (Dirmeyer *et al*., 2006). This analysis has been validated and shown to be superior to any individual model in terms of its representation of soil moisture variations (Guo *et al*., 2007 and Gao and Dirmeyer, 2006). However, an explicit evaluation of the evapotranspiration against direct or complementary observations has not been performed. The bulk of the GSWP-2 output data, including baseline simulations, multi-model analyses, and sensitivity studies, are reported at a daily interval. There exist also sub-diurnal outputs at 3-hour intervals from the models, which were logged (as instructed by the GSWP-2 exercise) during the last year (1995) for all the baseline simulations.

Table 1. List of model acronyms used in this study. Refer to Dirmeyer *et al*. (2006) for further model details.

Acronym (for this study)	GSWP-2 Model Information
CLM2-TOP	CLM2-TOP: University of Texax, USA
HYSSIB	HY-SSiB: NASA/GSFC, USA
ISBA	ISBA: Météo-France/CNRM, France
LaD	LaD: NOAA/GFDL, USA
MOSAIC	Mosaic: NASA GSFC/HSB, USA
MOSES2	MOSES2: Met Office, United Kingdom
NOAH	Noah: NOAA/NCEP/EMC, USA
NSIPP	NSIPP-Catchment: NASA GSFC/GMAO, USA
ORCHIDEE	ORCHIDEE: ISPL, France
SiBUC	SiBUC: Kyoto University, Japan
SSiBCOLA	SSiBCOLA: IGES/COLA, USA
SWAP	SWAP: Russian Academy of Sciences/IWP, Russia
VISA	VISA: University of Texas, USA

Another essential component of GSWP-2 involves a suite of sensitivity studies (**Table 2**) by the participating LSSs where forcing data or boundary conditions are altered to examine the response of the models to uncertainties in those parameters. GSWP-2 provides various alternates of meteorological forcing variables and land surface parameters for designated sensitivities studies (IGPO, 2002). Participation in the sensitivity studies by each modeling group was optional. **Table 3** lists all the sensitivity simulations that the models performed and outputs collected. These simulations include substitutions to precipitation, radiation, all meteorological forcing, and vegetation properties. The sensitivities of different LSSs to uncertainties in the precipitation data (i.e. runs P1, P2, P3, P4, and PE) specifically address the impacts of bias correction by hybridization, choice of different reanalysis products, the range in observational

Table 2. Description of various GSWP-2 sensitivity experiments (meteorological forcing and vegetation data sets used in the sensitivity experiments are the same as the B0 baseline integration unless otherwise specified below).

Sensitivity Experiment	Description of meteorological forcing and vegetation data sets
B0	Tair and Qair: NCEP/DOE hybridized with CRU; Wind: NCEP/DOE; SWdown and LWdown: SRB; PSurf: NCEP/DOE with altitude (EDC topography) correction; Rainf, Rainf_C, and Snowf: NCEP/DOE hybridized with GPCC gridded gauge analysis, corrected for wind-caused gauge undercatch, and blended with GPCP where the gauge density is low; Vegetation: observed inter-annually varying monthly vegetation parameters;
M1	All original NCEP/DOE meteorological data (no hybridization with observational data)
M2	All original ECMWF (ERA-40) meteorological data (no hybridization with observational data)
P1	Original ERA-40 precipitation (no hybridization with observational data)
PE	ERA-40 precipitation hybridized with GPCC gridded gauge analysis, corrected for wind-caused gauge undercatch, and blended with GPCP where the gauge density is low;
P2	NCEP/DOE precipitation hybridized with GPCC gauge analysis and corrected for wind-caused gauge undercatch
P3	NCEP/DOE precipitation hybridized with GPCC gauge analysis only
P4	Original NCEP/DOE precipitation (no hybridization with observational data)
R1	Radiation from NCEP/DOE reanalysis
R2	Radiation from ERA-40 reanalysis
R3	Radiation from ISCCP [*Rossow and Zhang, 1995*]
I1	Climatological annual cycle of vegetation parameters

estimates, and rain-gauge under-catch. The radiation series (i.e. runs R1, R2, and R3) provide a similar evaluation for the impact of the systematic differences between the reanalyses' and ISCCP radiation. The all-meteorological study (i.e. runs M1 and M2) gives the broadest assessment as to the impact of differences between the two reanalyses. The sensitivity with vegetation properties (run I1) examines the impact of the interannual variability versus mean seasonal cycle of vegetation phenology. Since reanalysis products are widely used as a proxy for true atmospheric conditions, these sensitivity studies have important implications, such that we can gauge the certitude of scientific results achieved using these data sets (i.e. for global hydrological cycle studies).

Table 3. Summary of conducted sensitivity experiments for each of the participating GSWP-2 models, with an "X" indicating that the simulation was performed.

	B0	**I1**	**M1**	**M2**	**P1**	**P2**	**P3**	**P4**	**PE**	**R1**	**R2**	**R3**
SSiBCOLA	X	X	X	X	X	X	X	X	X	X	X	X
NSIPP	X	X	X	X	X	X	X	X	X	X		X
SWAP	X	X	X		X	X	X			X		
NOAH	X	X			X	X	X		X	X		
MOSES	X						X			X		

2.2 Observations

2.2.1 Global-scale Data

For our global-scale assessment of the GSWP-2 evapotranspiration estimates, we draw upon data and results from a recent global water budget analysis (Schlosser and Houser, 2007). The SH07 study combined global fields of precipitation, evaporation (separate land and ocean estimates), and water vapor to perform an atmospheric-based water budget assessment via six core data sets:

- The Global Precipitation Climatology Project (GPCP) Version 2 (Adler *et al.*, 2003)
- The Climate Prediction Center (CPC) Merged Analysis of Precipitation (CMAP, Xie and Arkin, 1997)
- Goddard Satellite-based Surface Turbulent Fluxes - Version 2 (GSSTF, Chou *et al.*, 2003)
- Hamburg Ocean Atmosphere Parameters and Fluxes from Satellite (HOAPS) data (Bentamy *et al.*, 2003)
- COLA Global Offline Land-surface Data (GOLD) sets (Dirmeyer and Tan, 2001)

- National Aeronautics and Space Administration (NASA) Global Water Vapor Project (NVAP, Vonder Harr *et al.*, 2003)

SH07 provides further details regarding these data sets, and the period of overlap between these datasets and the GSWP-2 data covers the years 1988-1995. Missing from the SH07 study was an explicit estimate of the uncertainty in the global land evapotranspiration, and therefore we will use the GSWP-2 results to provide a scatter of land evapotranspiration within the global water balance. In addition, we have augmented the data collection of SH07 in our analysis to include the latest version of the HOAPS ocean evaporation estimate (HOAPS3, http://www.hoaps.zmaw.de/) as well as a gap-filled version of CMAP using the NCAR Reanalysis precipitation values *(*CMAPr, provided by the NOAA/OAR/ESRL PSD, Boulder, Colorado, USA, from their web site at http://www.cdc.noaa.gov/).

2.2.2 Field Data

To evaluate the performances of evapotranspiration simulations from various land surface models as well as the quality of the precipitation forcing in GSWP-2, observations of precipitation and evapotranspiration (or latent heat flux) have been collected. Four sites have been identified for this study, whose data temporally overlap the GSWP-2 period. **Table 4** summarizes the characteristics of each data set used in this study. Some of these observational sites have a relatively short record of overlap with the GSWP-2, but they all have at least one year of data for comparison. The GSWP-2 grid values corresponding to the individual validation site have been extracted from the various model baseline simulations, multi-model analyses, and sensitivity experiments for evaluation with the observations.

Our most complete source of field data (in terms of temporal domain) is from the North Appalachian Experimental Watershed (NAEW, Harmel *et al.*, 2007), which is located near Coshocton in east central Ohio, an unglaciated portion of the state with rolling uplands. Its 1050-acre outdoor laboratory facility is operated by the U.S. Department of Agriculture (USDA) – Agricultural Research Services (ARS). The NAEW consists of a network of 22 instrumented watersheds, 11 large lysimeters, meteorological stations, and rain gauges for surface- and ground-water hydrology and water quality studies. The experimental watersheds with natural setting range in size from 1 to 300 acres and five of them are larger than 40 acres. The NAEW is one of only two hydrologic stations worldwide with over 60 years of continuous data collected from small watersheds and groundwater lysimeters. The Coshocton site was selected because it represented land conditions prevalent in many states in the Appalachian Region. There are 11 active rain gages distributed over the watershed area. Provisional analyses (not shown) indicate little spatial variability in the watershed precipitation with the temporal cross-correlations among the 60-year daily precipitation time series of 11 rain gages all larger than 0.95. Therefore, all these rain gauges are averaged to approximately represent the scales of the GSWP-2 LSS grid box at 1° resolution. There is only one weighing lysimeter to record the evapotranspiration. All the observations are aggregated to monthly interval for comparisons with GSWP-2 model simulations.

The second source of data comes from the FLUXNET network of micrometeorological tower sites (Baldocchi *et al.*, 2001), designed primarily to measure the exchanges of carbon dioxide, water vapor, and energy between terrestrial ecosystem and atmosphere. Specifically, the Level 3 data from the AmeriFlux regional networks are available for a number of years overlapping with the GSWP-2 period. This level of data have gone through consistency checks for units, naming conventions, reporting intervals, and formatting with quality flag assigned, but without filling in the missing values. We have chosen to use the unfilled instead of gap-filled data because of questionable quality of the model-based gap-filling procedure (Bill Munger, 2007, personal communication). Three sites have multiyear records of fluxes and precipitation within the GSWP-2 period. Data from the Harvard Forest Environmental Measurement Site (EMS) was established in October 1989 but the quality-assured data set started in 1992. Data collection at the Northern Study Area Old Black Spruce site (NOBS), located near Thompson, Manitoba, started in 1994 during the BOREAS experiment in the northern boreal forests of Canada. The meteorological tower in the Walker Branch Watershed near Oak Ridge, Tennessee was established in 1979, and flux data collection started in 1994.

There are gaps in the precipitation data of 1994 at the BOREAS NOBS site. One reason is that rain gauge did not seem to work well for snow, which is a major part of the precipitation at this site. As a result, the data gaps are not random and measurements are somewhat biased towards convective precipitation (Allison Dunn, 2007, personal communication). Therefore, in this study, we use precipitation data from nearby Thompson Airport, Manitoba, Canada (55.8N, 97.86W, 223.1m elevation, http://www.climate.weatheroffice.ec.gc.ca/climateData/canada_e.html) to complement the

Table 4. Site characteristics of each field data selected in the local validation of this study. Map labels used in Figure 5 are also indicated. An "A" is used for all ARM stations due to close proximity.

Site (Map Label)	Latitude Longitude Elevation	Site Vegetation	Vegetation Type	Measurements (sampling interval)	Time domain
NAEW (C)	40.37°N 81.79°W 243 m	Rangeland	SiB, BATS, IGBP: Broadleaf deciduous	Lysimeter (daily) Precipitation (irregular, frequent than daily)	1986 ~1995
Harvard Forest EMS (H)	42.54°N 72.17°W 340 m	Temperate Deciduous	SiB, BATS, IGBP: Broadleaf deciduous	Water vapor eddy covariance flux (hourly) Precipitation (daily)	1992 ~1995
BOREAS NOBS (B)	55.88°N 98.48°W 259 m	Needleleaf evergreen	SiB, BATS, IGBP: Needleleaf evergreen	Latent heat flux (30 mins) Precipitation (daily)	1994 ~1995
Walker Branch (W)	35.96°N 84.29°W 372 m	Deciduous broadleaf temperate	SiB: Deciduous and Evergreen BATS and IGBP: Mixed forest	Latent heat flux (30 mins) Precipitation (daily)	1995
ARM E8 Coldwater (A)	37.33°N 99.31°W 664 m	Rangeland (grazed)	SiB: C3 Grass BATS: Cropland IGBP: Cropland	Latent heat flux (30 mins) Precipitation (30 mins)	1994 ~1995
ARM E9 Ashton (A)	37.13°N 97.27°W 386 m	Pasture	SiB: C3 Grass BATS: Cropland IGBP: Cropland		
ARM E13 Lamont (A)	36.61°N 97.49°W 318 m	Pasture and wheat	SiB: C3 Grass BATS: Cropland IGBP: Cropland		
ARM E15 Ringwood (A)	36.43°N 98.28°W 418 m	Pasture	SiB: Groundcover BATS: Short grass IGBP: Grassland		
ARM E20 Meeker (A)	35.56°N 97.00°W 309 m	Pasture	SiB: Groundcover w/trees and shrubs BATS: Forest/Field IGBP: Woody Savanna		

available flux measurements for the evaluation exercise. The Thompson site reports both rainfall (amount of all liquid precipitation such as rain, drizzle, freezing rain, and hail) and snowfall (amount of frozen/solid precipitation such as snow and ice pellets). The sum of rainfall and the water equivalent of the snowfall is used here.

During the years overlapping with the GSWP-2 period, data collection in all three AmeriFlux sites experienced technical difficulties and instrumentation failure. As a result, temporal coverage for the relevant flux measurements is, at times, irregular (although it has improved in recent years). For our analyses, these gaps in half-hourly or hourly data are addressed in the following manner. We first derive the climatology of diurnal cycle for each calendar month based on the available observations of that month. Then we fill in missing measurements with the derived month-specific diurnal cycle climatology. The hourly or half-hourly data are aggregated to 3-hourly (1995 only), daily, and monthly whenever necessary for comparisons with the model simulations.

The U.S. Department of Energy operates the Atmospheric Radiation Measurement (ARM) Program (Ackerman and Stokes, 2003). In particular, the southern Great Plains site consists of a central facility and a number of Extended Facilities across a large area of Oklahoma and southern Kansas, each having instrument clusters to measure radiation, near-surface meteorology and surface fluxes. For our study, data from the Energy Balance Bowen Ratio (EBBR; Cook 2005) system and the Surface Meteorological Observation System (SMOS) at the extended facility is appropriate. The EBBR uses observations of net radiation, soil surface heat flux, and the vertical gradients of temperature and relative humidity to estimate the vertical heat flux at the local surface. The SMOS mostly uses conventional in situ sensors to obtain averages of surface wind speed, wind direction, air temperature, relative humidity, barometric pressure, and precipitation at the 1-minute, 30-minute, and daily intervals. Data archives of 10 stations exist for the EBBR and of 5 stations for the SMOS during the 1994 ~ 1995 period. Herein, we use the A1-level data (Table 4), in which calibration factors are applied. The data are provided as 30-minute averages, and we apply the same procedure as for the FLUXNET (month-specific diurnal cycle climatology) to fill in any missing measurements. The resulting half-hourly data is further averaged to 3-hourly (1995 only), daily, and monthly for consistency with the model output from the GSWP-2.

3. ANALYSIS

3.1 Global-scale Evaluation

3.1.1 Annual Mean and Variability

For the global, mean annual estimates of evapotranspiration, the GSWP-2 models exhibit a range of values in the B0 simulation of 49 to 75 trillion metric tons/year (TMT/year or 10^{15}

kg/year). The model-mean value is 65 TMT/year (**Figure 1a**) with a notable clustering of model results (i.e. 7 of the 13 models are within ±2.5%). In terms of a unit-area flux, 1 TMT (= 10^{15} kg) is equivalent to 6.67 mm depth of water distributed equally across all land areas, and thus the model-mean, global land annual evapotranspiration flux is 434 mm/year or 1.19 mm/day. The

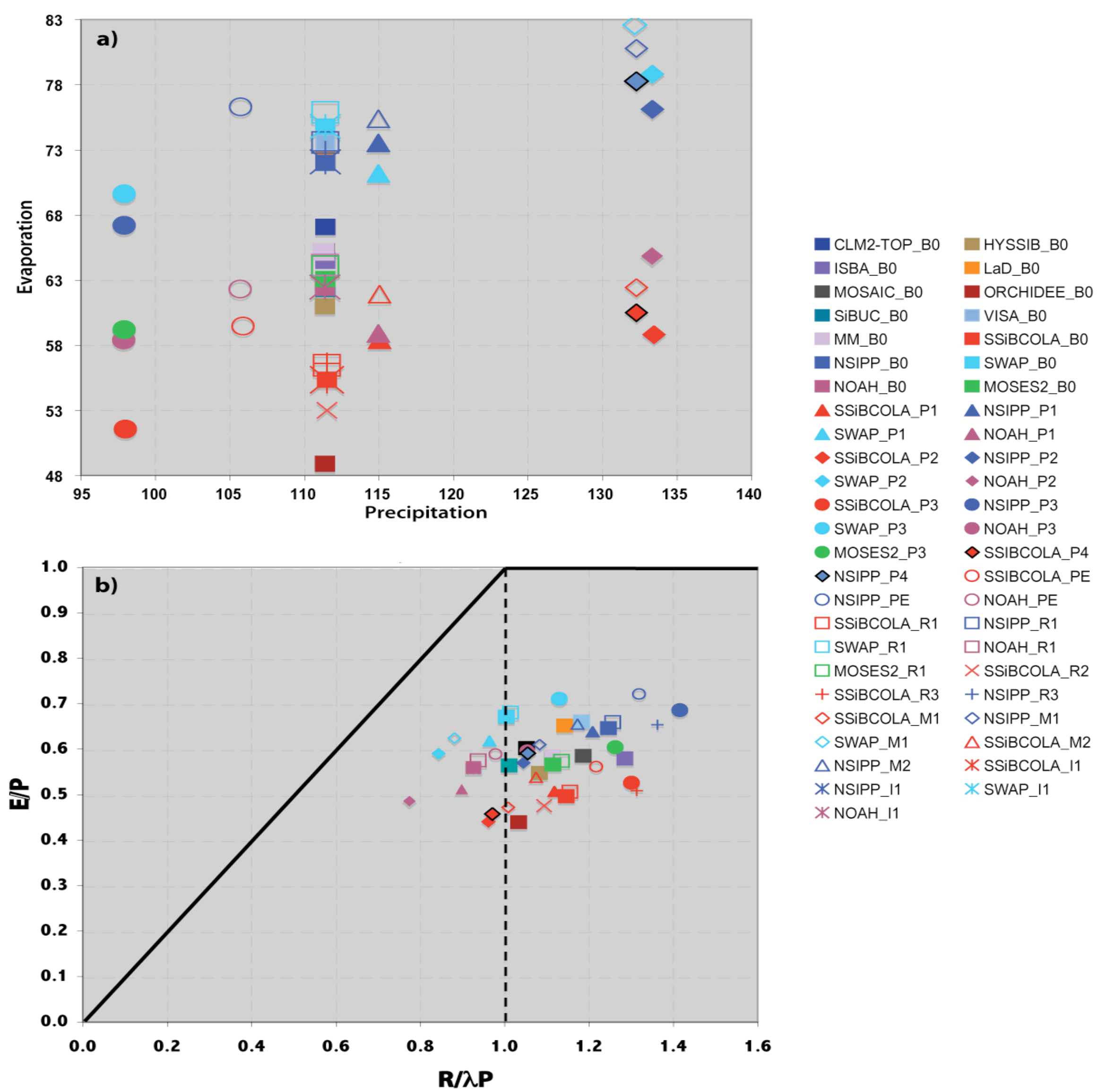

Figure 1. (a) Scatter plot of GSWP-2 global annual mean land evapotranspiration against global precipitation of the various simulation experiments. Units are given in trillion metric tons (TMT = 10^{15} kg) per year. (b) Budyko diagram of GSWP-2 simulations showing comparison of net radiation and evapotranspiration, scaled by precipitation. Results are based on global, mean annual values.

inter-model scatter seen in the baseline simulations is largely preserved in the sensitivity experiments, even though fewer of the participating models conducted these runs (but the range between SSiBCOLA and SWAP remains fairly constant across all sensitivity runs). The total range (i.e. highest-lowest) of the baseline simulations of global evapotranspiration is 26 TMT/year. With respect to the modern-era observationally based global water budget assessments by SH07 this range is comparable to the global imbalance of precipitation and evaporation (about 24 TMT/year or 5% of the global precipitation rate). The range is considerably larger than the interannual variability of any particular GSWP-2 model's annual evapotranspiration, which is about 0.65 TMT/year (taken as the value of σ_{total} from Table 4 of Dirmeyer *et al.*, 2006). Further, the choice of atmospheric forcing (discussed in more detail below) is seen to shift the model-mean estimate by as much as ±5 TMT/year (or about ±8% of the baseline simulation model-mean value) and that the largest shifts result from changes in the precipitation forcing. Nevertheless, the results indicate that model structure plays a more important role than uncertainty in atmospheric forcing for these global evapotranspiration estimates.

Table 5. The residual calculations of annual ocean evaporation (denoted by asterisk) using the global GPCP and CMAP precipitation rates (Schlosser and Houser, 2007) together with the GSWP-2 land evaporation plus the Antarctica evaporation (Loewe, 1957). Residual error of ocean evaporation is calculated using sampling errors from GPCP and CMAP (Schlosser and Houser, 2007) and the standard deviation of the annual GSWP-2 evaporation (Dirmeyer *et al.*, 2006). Units are in kg/year.

Land Evaporation		**Global Precipitation**	
Antarctica	**GSWP-2**	**GPCP**	**CMAP**
7.41E+14	6.51±0.08E+16	4.9±0.15E+17	4.94±0.09E+17
	Ocean Evaporation		
GPCP – GSWP-2*	**CMAP – GSWP-2***	**HOAPS3**	**GSSTF2**
4.24±0.15E+17	4.28±0.09E+17	3.95E+17	4.30E+17

We can use the GSWP-2 model-mean estimate of global land evaporation (and the inter-model standard deviation) together with the global precipitation estimates and sampling error (from SH07), to obtain as a residual an estimate for global, mean ocean evaporation (**Table 5**). To perform this calculation, an estimate for the evaporation rate over Antarctica (not considered in the GSWP-2 simulations) is also required. For this, we used the approach as given by Loewe (1957), which provides evaporation flux rates as a function of latitude, and we integrated these rates over the Antarctic land area. Inclusion of this Antarctic flux estimate increases the global GSWP-2 evapotranspiration by about 1% (Table 5). Based on these estimates, we find that the implied mean evaporation from the global oceans to be 426 ± 12 TMT/year. The GSWP-2 residual estimate is more consistent to the GSSTF2 estimate (= 430 TMT/year) as opposed to the HOAPS estimate (= 395 TMT/year). However, uncertainty bounds for both the GSSTF2 and HOAPS estimates are not available (and beyond the scope of this study), and thus an unequivocal assessment in this regard is not possible. However, it is encouraging that the GSWP-2 residual falls in between the more explicit and widely used estimates of global ocean evaporation rates.

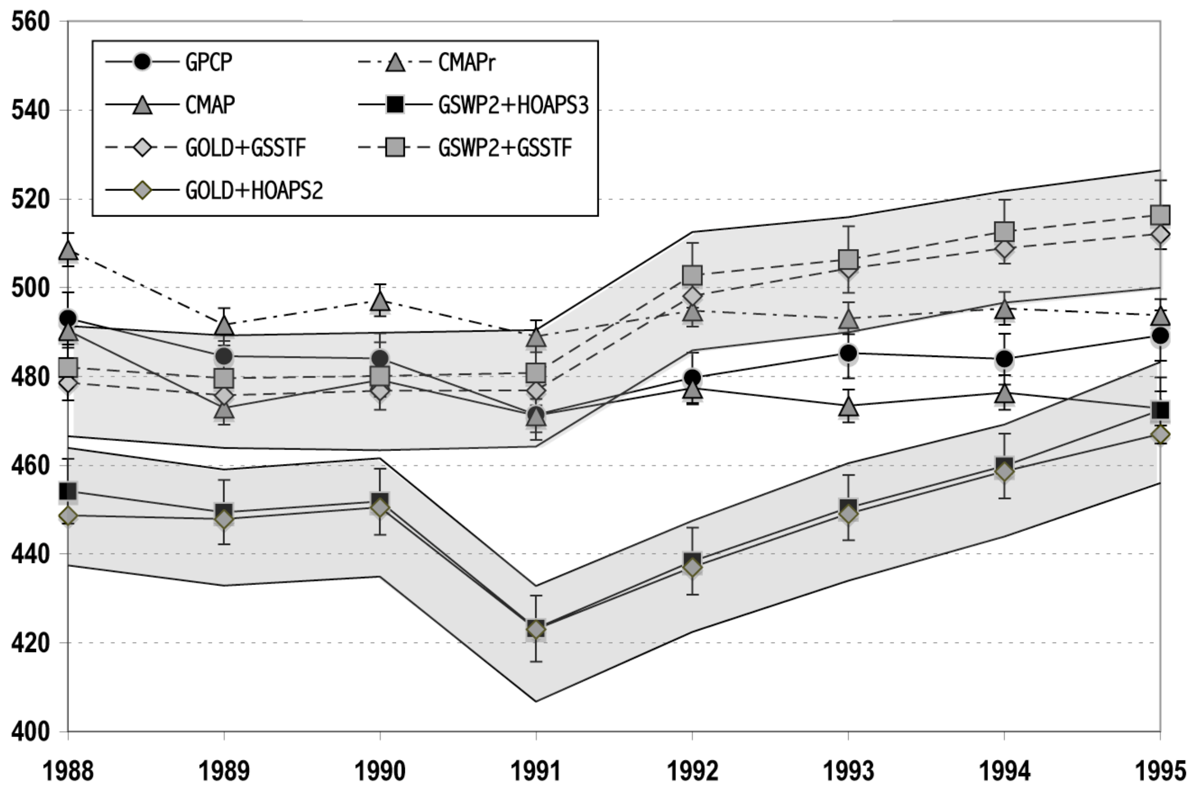

Figure 2. Annual timeseries of global evaporation using combinations of various datasets (see text for details) as well as the global precipitation from GPCP and CMAP (that also includes a gap-filled CMAP product, CMAPr). Unit is TMT/year. The gray shaded region indicates the extent of the GSWP-2 model scatter about the global evaporation estimate (using the GSWP-2 model-mean for land evaporation).

Looking further at the disparity among these global-scale evaporation estimates (**Figure 2**), the spread in the annual land estimates from all of the participating GSWP-2 models (13 B0 simulations) is about half of (and never greater than) the difference in the GSSTF and HOAPS ocean estimates. Considering that the ocean covers about twice as much of the Earth's surface as the land, this twofold increase in the difference between the global ocean evaporation rates (compared to the GSWP-2 range) is not surprising. Yet, it is worth noting that, generally speaking, the two ocean estimates considered in this study use very similar bulk aerodynamic algorithms, but with different sources of atmospheric data to satisfy their formulae requirements, whereas the GSWP-2 spread is a result of structural differences amongst the models, but each one forced by identical atmospheric conditions. There is also a notable increase in the spread of the global evaporation estimates (constructed by the GSWP-2 B0 estimates and the ocean evaporation algorithms) starting in 1991. As noted in SH07 (see their Figure 8), this is primarily a result of a sharp decrease in the HOAPS humidity gradient fields (derived from AVHRR data) throughout the tropics following the Mt. Pinatubo eruption. Then, the persistently smaller values of HOAPS (compared to the GSSTF estimate) in subsequent years are primarily attributed to weaker tropical wind fields (Figure 8 of SH07). Nevertheless, in choosing any of the two ocean evaporation data sets considered (and widely used in the climate research community), the GSWP-2 scatter cannot account for the global imbalance between evaporation and precipitation for all years considered in this study, which according to SH07, should only be on the order of 10^{14} kg as indicated by annual global water vapor tendencies (Figure 6 of SH07).

3.1.2 Mean Annual Cycle

Among the more considerable discrepancies amongst the global water budget terms considered in the SH07 study is seen in the depiction of the mean annual cycles. For this study, none of the combinations of water flux terms (i.e. precipitation and evaporation), that include the addition of the GSWP-2 estimates, were able to produce global E-P values that matched consistently with observed variations in global atmospheric water vapor storage (**Figure 3**). When considering the GSWP-2 model-mean estimate for global land evapotranspiration, as well as the model spread about the mean (Figure 3, gray shaded region), only marginal consistency can be inferred between monthly tendencies of global E-P and water vapor storage during the Northern Hemisphere warm season months. However, for the remaining months of the annual cycle, none of the GSWP-2 model results can account for the substantial bias that exists between global E-P and the monthly changes in atmospheric water storage. Additionally, the relative maximum of net atmospheric water gain (occurs in June) is one month earlier than that inferred from the E-P estimates (occurs in July), and similar (but mixed) results are seen for the relative minimum. Moreover, all E-P estimates show notably higher magnitudes of their annual cycles as compared to the atmospheric water storage changes. The inconsistent timing of the relative maxima/ minima and magnitude of the E-P annual cycle are closely aligned with the corresponding features of the GSWP-2 global evapotranspiration (**Figure 4**). This does not necessarily prove that all the GSWP-2 estimates are wrong, but does implicate that its interplay with observationally based estimates of global precipitation and ocean evaporation is not consistent with observations of global water vapor.

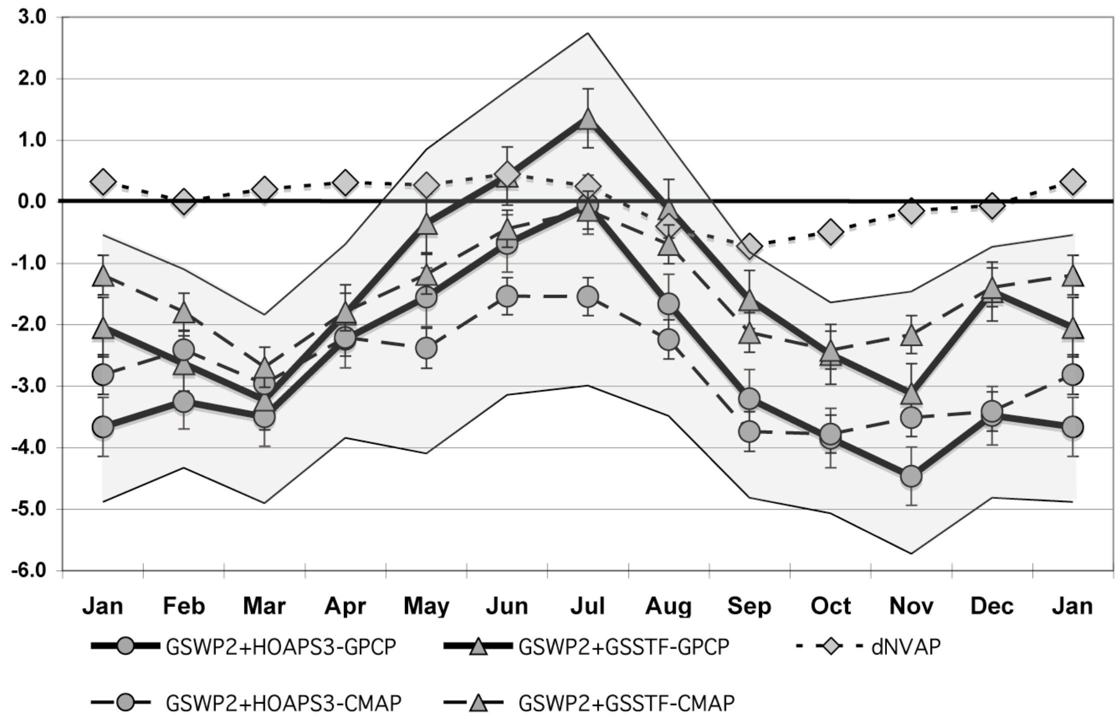

Figure 3. Global mean annual-cycles (1988-1995) of evaporation minus precipitation (E-P) for selected combinations of evaporation (from Figure 2) and precipitation estimates as well as corresponding monthly change in total atmospheric water vapor storage. The gray shaded region indicates the total range of the E-P estimates from the GSWP-2 model collection. Units are in TMT/month.

The systematically lower values of E-P (and in some months opposite sign) to atmospheric water vapor changes, particularly from October through May, imply substantial biases between E and P and/or a measurement error in water vapor. Unfortunately, the uncertainty estimates of the monthly atmospheric water vapor were not readily obtainable for evaluation in this study.

Nevertheless, given these large systematic differences (between 2 to 5 TMT depending on the choice of E and P estimates), the measurement error in global water vapor would need to be on the order of 20% (i.e. noting that from SH07 Figure 6, global water vapor storage is ~10 TMT or 10^{16} kg) in order to partially explain these discrepancies. However, in doing so, this would also consume most (if not all) of its annual cycle signal (seen in Figure 3). Further, in the absence of water vapor trends, the annual mean of the E-P tendencies should be zero. The NVAP observations indicate a decrease in global water vapor storage of ~0.03 TMT through the 1988-1995 period (Figure 6 of SH07). While this trend implies a mean negative rate (or bias) of global E-P through the period, it is orders of magnitude smaller than the systematic bias of

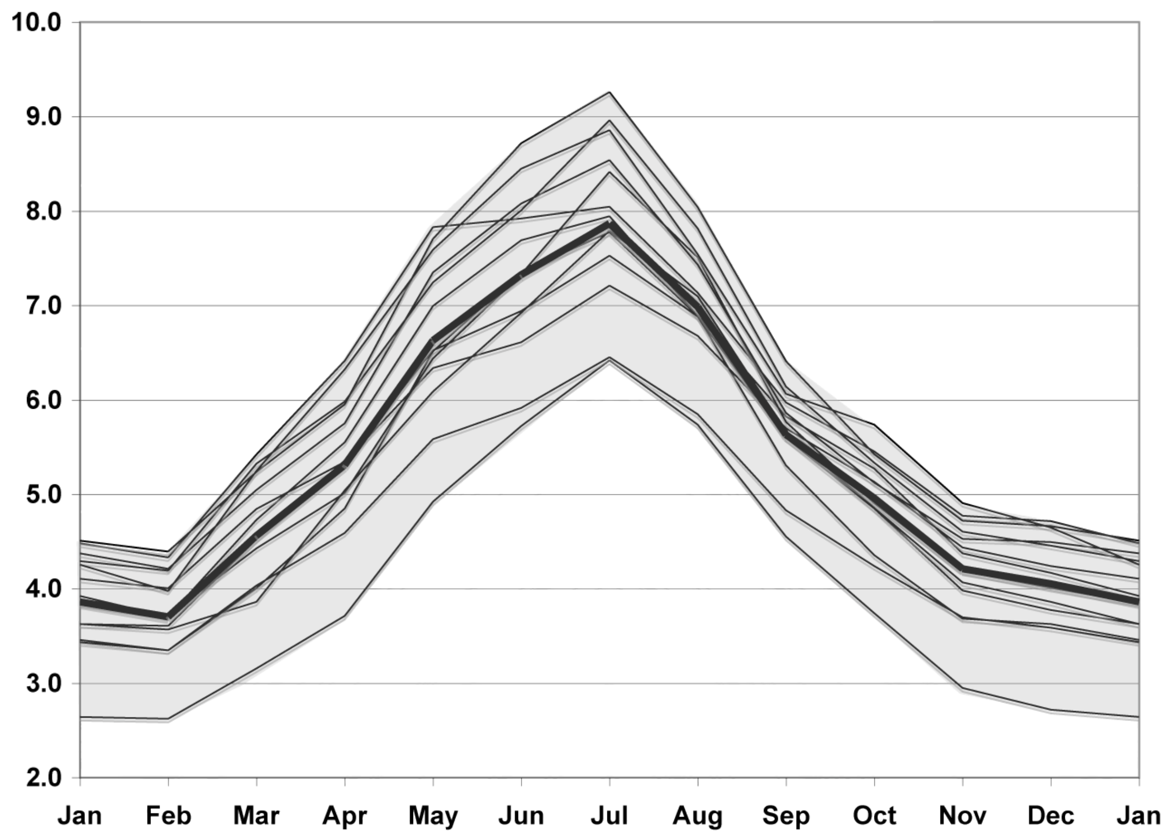

Figure 4. Global mean annual cycles (1986-1995) of evapotranspiration from all the GSWP-2 baseline simulations (in TMT/month). The heavy curve and light curves indicate the GSWP-2 model-mean and individual model results, respectively. The total scatter of the GSWP-2 models is highlighted in gray.

approximately 2 TMT/month seen here. In addition, the range of GSWP-2 evapotranspiration (Figure 4) cannot account for this inconsistency throughout the entire annual cycle. Thus, refinements in the global precipitation and ocean evaporation estimates and error estimates of water vapor measurement are needed to clarify these inconsistencies.

3.2 Sensitivity to Precipitation and Radiation Forcing

Taking advantage of the suite of sensitivity experiments (Table 2) run by a subset of the GSWP-2 models for which baseline runs were also submitted (Table 3), we assess the global-scale sensitivity of evapotranspiration to two primary atmospheric forcing terms, precipitation and net radiation (R). For every model, we calculate the change in global evapotranspiration with respect to all combinations of changes in the two forcing terms considered (**Table 6**). These

Table 6. The differences between the precipitation and radiation sensitivity simulations as well as the baseline (B0) experiment. A * indicates that the difference between the two runs are from a single modification or substitution of precipitation.

Experiment	Relative Differences
R1-B0	NCEP-DOE *versus* SRB radiation
R2-B0	ERA-40 *versus* SRB radiation
R2-R1	ERA-40 *versus* NCEP-DOE radiation
R3-B0	ISCCP *versus* SRB radiation
R3-R1	ISSCP *versus* NCEP-DOE radiation
R3-R2	ISCCP *versus* ERA-40 radiation
P4-P3*	Add GPCC gauge analysis to original NCEP-DOE
P3-P2*	Add wind undercatch correction to NCEP-DOE w/ GPCC gauge analysis
P2-B0*	Add GPCP relaxation to complete the NCEP-DOE hybridization
P3-B0	Add wind undercatch correction and GPCP relaxation to complete the NCEP-DOE hybridization
P4-B0	Original *versus* hybridized NCEP-DOE
P4-P2	Add wind undercatch correction and GPCC gauge analysis to original NCEP-DOE
P1-PE	Original *versus* hybridized ERA-40
P1-B0	Original ERA-40 *versus* hybridized NCEP-DOE precipitation
PE-B0*	Hybridized ERA-40 *versus* hybridized NCEP-DOE precipitation
P4-P1*	Original NCEP-DOE *versus* original ERA-40 precipitation
P4-PE	Original NCEP-DOE *versus* hybridized ERA-40 precipitation
P2-P1	Hybridized NCEP-DOE w/o GPCP relaxation *versus* original ERA-40
P3-P1	NCEP-DOE w/ GPCC analysis only *versus* original ERA-40
P2-PE	Hybridized NCEP-DOE w/o GPCP relaxation *versus* hybridized ERA-40
P3-PE	NCEP-DOE w/ GPCC analysis only *versus* hybridized ERA-40

sensitivities, $\frac{d\overline{E}}{d\overline{P}}$ and $\frac{d\overline{E}}{d\overline{R}}$ (**Table 7**, and overbar denotes global area-weighted mean) are, in principle, calculable given that each of the sensitivity experiments changes these forcings one at a time in a consistent fashion. As will be shown, however, care must be taken in the interpretation of these results.

The precipitation sensitivity results provide 5 model samples, with 4 of the models reporting runs for at least 3 of the 5 possible experiments (i.e. runs P1 to PE, see Table 3). First, we focus on the runs that change - but do not substitute - the NCEP-DOE precipitation (used in the B0

Table 7. Global evapotranspiration (E) sensitivities, $\frac{d\overline{E}}{d\overline{P}}$ and $\frac{d\overline{E}}{d\overline{R}}$, as calculated based on 10-year averaged global mean values from the radiation (R) and precipitation (P) sensitivity experiments. Radiation (Wm^{-2}) is converted to mm/day (Dirmeyer *et al.*, 1999, 1 Wm^{-2} = 0.03455 mm/day).

Sensitivity	Experiment	Model				
		SSiB	**NSIPP**	**SWAP**	**MOSES2**	**NOAH**
$\frac{d\overline{E}}{d\overline{R}}$	R1-B0	0.24	0.31	0.21	0.19	0.38
	R2-B0	0.27				
	R2-R1	0.26				
	R3-B0	0.02	0.03			
	R3-R1	-0.03	-0.03			
	R3-R2	0.09				
$\frac{d\overline{E}}{d\overline{P}}$	P4-P3	0.26	0.32			
	P3-P2	0.21	0.25	0.26		0.18
	P2-B0	0.16	0.18	0.18		0.11
	P3-B0	0.28	0.36	0.39	0.29	0.30
	P4-B0	0.25	0.30			
	P4-P2	-1.55	-2.00			
	P1-PE	-0.11	-0.29			-0.37
	P1-B0	0.86	0.41	-1.04		-0.97
	PE-B0	-0.73	-0.74			0.01
	P4-P1	0.12	0.27			
	P4-PE	0.04	0.07			
	P2-P1	0.02	0.14	0.41		0.32
	P3-P1	0.40	0.37	0.09		0.03
	P2-PE	-0.02	-0.01			0.09
	P3-PE	1.02	1.17			0.50

run), which are runs P2, P3, and P4. For the most part, the evapotranspiration sensitivities in this group (denoted by medium-shaded gray boxes in Tables 6 and 7) show a reasonable consistency in the sign and magnitude. The notable exception is found for the P4-P2 result, which shows an exaggerated negative sensitivity to a small change in global precipitation from the NCEP-DOE product as a result of the GPCC analysis plus the wind under-catchment adjustment. Recent evidence suggests that the wind under-catchment adjustment is likely to have been excessive and erroneous, resulting in questionable quality of the P2 precipitation field (Decharne and Douville, 2006 – and see next section). We also note that, for all GSWP-2 models performing these sensitivity runs, the evapotranspiration sensitivities obtained from the P2-B0 change (i.e. effect of GPCP blending at low gauge density) consistently show the lowest, non-negative value compared to all other NCEP-DOE precipitation modifications (i.e. excluding *substitution* with the ERA-40 precipitation). In view of these results, we must call into question the sensitivity quantifications that result from the P2 simulations.

What is perhaps more striking is that the sensitivities obtained from either the P1 or PE runs, which *substitute* the NCEP-DOE with the ERA-40 precipitation (denoted by the darkest-shaded gray boxes in Tables 6 and 7), show a wide ride of values with no apparent consistency or clustering. For these P1 and PE runs, the consistency of the substituted ERA-40 precipitation (hybridized or not) with the remaining meteorological fields[1] (i.e. radiation, surface-air temperature, winds, humidity, and air pressure) of the NCEP-DOE product is not assured. In other words, we are referring to the condition in which the timing, duration, and/or amount of (ERA-40) precipitation at any grid cell may not necessarily correspond to the (NCEP-DOE) radiation or atmospheric state variables (noted above). Therefore, it is reasonable to expect that any degree of inconsistency between the precipitation and remaining meteorological fields will cause spurious sensitivities and inconsistent behavior from the models (and seen in these results).

For the radiation sensitivity runs, we have a much smaller sample size of model results (Table 3). Nevertheless, we are able to make some characterizations among the modeled evapotranspiration sensitivities obtained. There is a notable difference between those sensitivities obtained with the ISCCP radiation substitution (denoted by the lightest-shaded gray boxes in Tables 6 and 7, mean value ~0.02, and with values of opposite sign) as opposed to those that result from a substitution of the B0 radiation fields with the ERA40 or NCEP reanalyses

[1] Hereafter, the term “remaining meteorological fields” will refer to all the atmospheric variables of the GSWP-2 forcing, but excluding the variable to which they are made reference.

radiation (mean value ~0.27). This disparity is not necessarily a reflection of differences in quality between any of the radiation products, but more likely consistency issues with the remaining meteorological data (as seen in the precipitation sensitivities). The B0 radiation field is a hybridization of the SRB data with the NCEP reanalyses (Dirmeyer *et al.*, 2006), while the R3 radiation field is a result of replacing the 3-hourly ISCCP product with no hybridization. Further, the R1 radiation is the NCEP reanalysis (used in the B0 hybridization) and the spatio-temporal patterns of the R1 and R2 radiation fields (not shown) are quite similar. While this does not quantify the extent of inconsistency in the R3 radiation (to the remaining meteorological variables), it does call into question its suitability for this sort of sensitivity assessment, and that further analysis (beyond the scope of this study) is warranted.

Therefore, in considering these results to characterize overall evapotranspiration sensitivity (to uncertainties in forcing), we consider only the simulations with NCEP-DOE precipitation, and we further exclude any runs that involve the wind under-catchment adjustment (i.e. the P2 run). For sensitivities with respect to radiation, we have chosen not to consider any of the R3 simulations given the aforementioned considerations. This leaves us with three combinations of runs to pool for sensitivity to precipitation (i.e. P4-P3, P3-B0, and P4-B0), and three combinations for sensitivity to net radiation (i.e. R1-B0, R2-B0, and R2-R1). As such, we find that global evapotranspiration's sensitivity to precipitation is 0.31, and the averaged sensitivity of evapotranspiration to radiation is approximately 0.27. The differences between these two mean sensitivities, while small, are consistent with the characterization that most of the GSWP-2 model simulations are marginally located on the "water limited" region of the Budyko curve (**Figure 1b**). However, looking further at the results for NOAH, we find that the sensitivity for evapotranspiration with respect to radiation is higher than that with respect to precipitation. This is, nevertheless, consistent with the positioning of its global evaporability and index of dryness values that place it predominantly within an "energy limited" categorization.

3.3 Inter-model Consistency

Our findings indicate that model structure plays a more substantial role than the meteorological inputs in the uncertainty of the GSWP-2 evapotranspiration estimates. Given this, we use a simple metric to quantify the degree to which the models perform consistently (or not) amongst themselves, as a guide for further model analyses and development. We perform point-wise temporal correlations (R) between all possible combinations of models for the B0

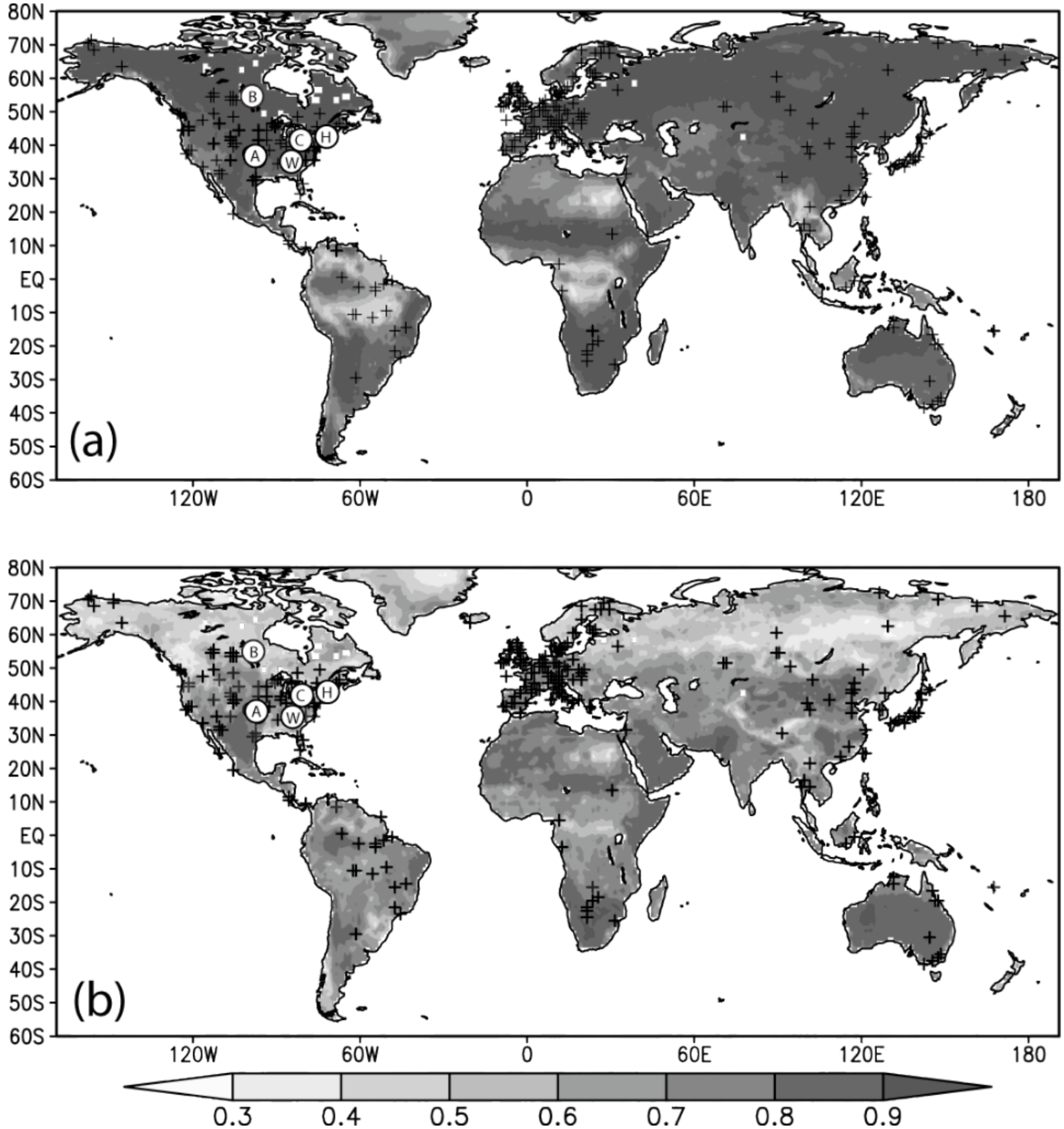

Figure 5. Global temporal consistency among the monthly evapotranspiration estimates of the GSWP-2 models. The (a) and (b) show the result with the annual cycle included and removed (i.e. anomaly correlation), respectively. Crosshairs and encircled letter indicate Fluxnet site and field data site used in this study, respectively.

simulations (a total of 78), and then take the average of these correlations. The strongest and most ubiquitous agreement amongst the models lies in the simulation of the annual cycle, with the most notable exception seen in tropical regions (**Figure 5a**). We find that the models show their largest and most widespread inconsistency among evapotranspiration variations at interannual timescales in many boreal regions (**Figure 5b**). However, consistency amongst the model simulations isn't necessarily indicative of their fidelity. For example, while the GSWP-2 models may agree in the timing of the seasonal maximum of global evapotranspiration (Figure 4), it may very well be contributing to an inconsistent seasonal variation between the global balance of E-P and atmospheric water vapor (Figure 3). As shown (Figure 5), regions where the GSWP-2 models indicate some of the largest model disparities (northern high latitudes) cannot be comprehensively evaluated due to absence of field data. Nevertheless, we are able to partially address these issues with a small collection of complementary field data (Table 4).

With the available field data, we calculate monthly correlation and root mean-square (RMS) error of the models against observed evapotranspiration, and display these two metrics as scatter plots (**Figure 6**). First and foremost, the results tend to corroborate the global assessment provided by Figure 5, that the ability of the GSWP-2 models to reproduce the observed inter-annual variability of evapotranspiration at higher latitude locations is not as robust. For the higher latitude sites (denoted by bigger, filled marks in the scatter plots), all correlations are reduced and a considerable portion of the correlations becomes negative when the annual cycle is removed from the timeseries (Figure 6b). While the RMS error is reduced in these cases, this is caused mostly by the fact that the magnitude of the inter-annual variations is smaller than the annual cycle (Figure 4b of Dirmeyer *et al*, 2006). For the lower latitude points (smaller marks in Figure 6) the results are qualitatively consistent – but the diminished correlations when removing the annual cycle are not as dramatic.

Evaluation of the models' monthly-averaged diurnal cycle of latent heat flux (**Figure 7**, excluding NAME, data not available) indicates that the models' collective inability to reproduce the observed values is greatest during the middle of the day during the warm-season months (April thru October) of 1995. Additionally, we find that at the Walker Branch site, the models show the greatest RMS error during April and May, while the Harvard Forest and Boreas sites indicate June as the most problematic month for the modeled estimates. For the aggregated ARM sites, June and July show the highest peaks in RMS error, but only marginally so compared to other months. Similar results (not shown) are found for the individual ARM site (Table 4) as well.

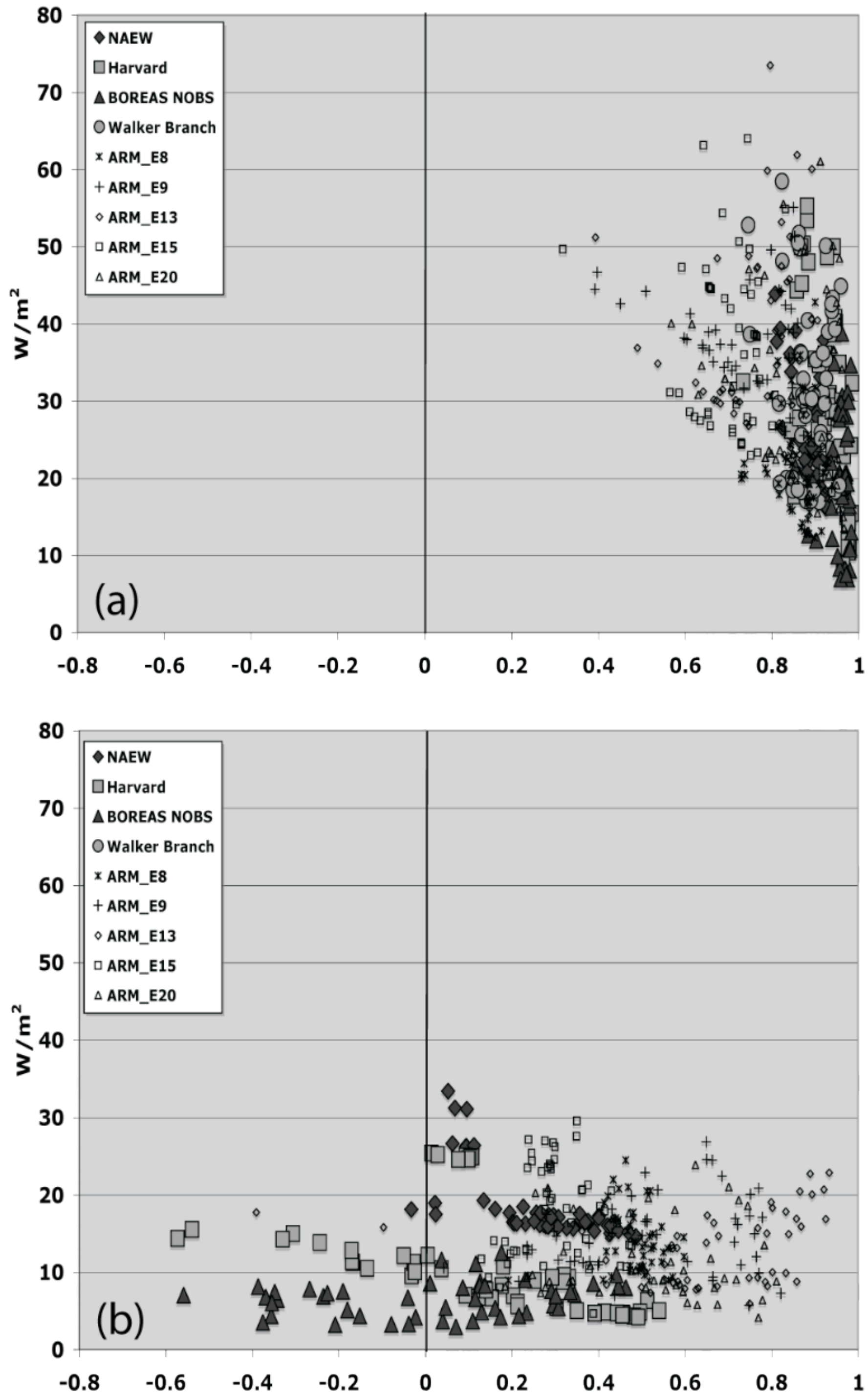

Figure 6. Scatterplots of root mean-square error (RMSE, W/m^2) versus temporal correlation of GSWP-2 modeled monthly latent heat flux with observations from a selection of field data collections (see text for details). The (a) and (b) show results with the mean annual cycle included and removed, respectively. The larger and filled plot marks indicate those field sites at (relatively) higher latitudes. Each point represents one simulation run of one model (including all baseline runs and all sensitivity runs from participating models).

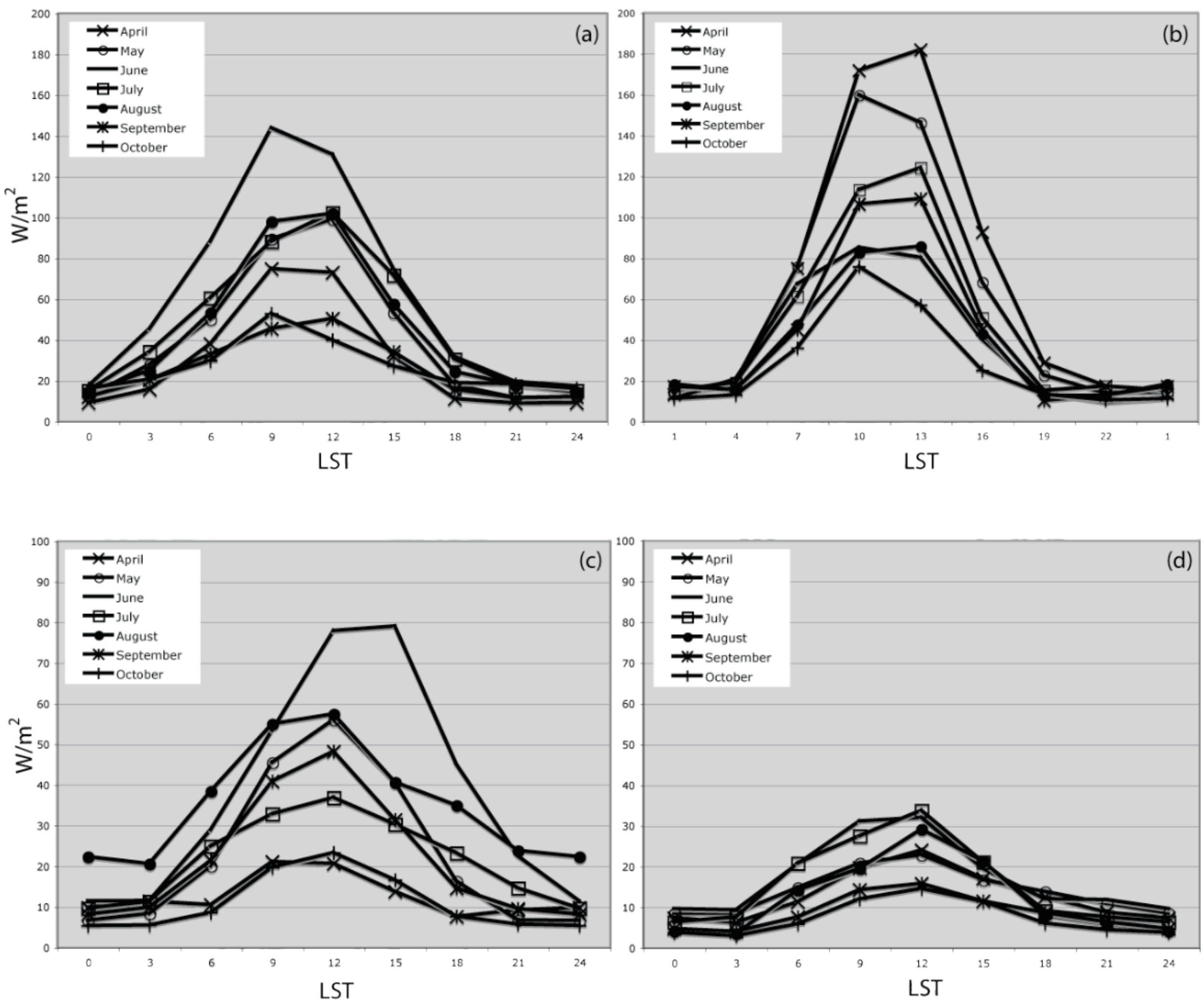

Figure 7. Monthly aggregates of the root mean-square error (RMSE) of simulated diurnal cycle of latent heat flux (W/m^2) averaged from all the B0 simulations of 1995 for (a) Harvard Forest, (b) Walker Branch, (c) BOREAS NOBS, and (d) ARM sites (Aggregate from all the ARM sites). Each curve represents the RMSE calculated against the observations by pooling each monthly-averaged diurnal cycle from the GSWP-2 B0 simulation.

Aside from model deficiencies, the errors shown between the models and the field observations may have also (partially) resulted from inconsistencies between the GSWP-2 grid-aggregate and field site conditions. The largest errors (in the diurnal cycles) are found at the Harvard Forest and Walker Branch sites, and it is also these sites where the locally observed vegetation conditions show a weaker correspondence (compared to the BOREAS and ARM sites) to the vegetation type described at the GSWP-2 model grids (Table 4). An additional concern is whether the local meteorological conditions at these field sites have any consistency to the corresponding GSWP-2 grid. Available precipitation data at these sites indicate that the baseline simulation (as well as the P1, P3, and PE sensitivity runs) show a strong degree of consistency in the seasonal to interannual variations (**Figure 8**), and therefore the evaporation errors at these sites is likely not a result of inconsistent precipitation provided by the GSWP-2 gridded data. Conversely, the correlation and/or RMS errors of the P2 and P4 precipitation to the field observations are considerably degraded, which is consistent with previous evaluations (Decharme *et al.*, 2006) and the interpretations of our own findings in the evapotranspiration sensitivities (Table 7).

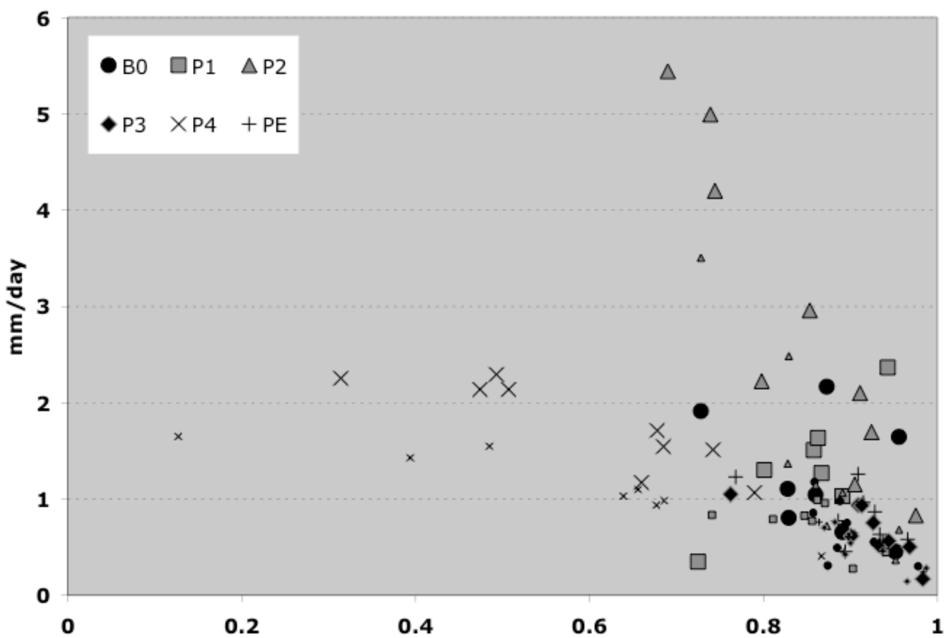

Figure 8. Scatter plot of the root-mean square error (RMSE, mm/day) of various GSWP-2 precipitaiton forcing data versus temporal correlation for the field sites selected for this study. The larger and smaller marks indicate results from the raw monthly timeseries and with the averaged annual cycle removed, respectively.

4. CLOSING REMARKS

We have assessed the simulations of global-scale evapotranspiration from the Global Soil Wetness Project Phase 2 (GSWP-2). We find that at a global scale the scatter of GSWP-2 evapotranspiration estimates can constrain a modern-era water budget assessment to within ±2.5%, but cannot unequivocally explain the imbalance between the global (i.e. ocean plus land) precipitation and evaporation annual variations. In addition, inconsistencies in the magnitude and timing of seasonal variations of the global water budget terms are also found to be associated with the GSWP-2 estimates. The scatter among the GSWP-2 global evapotranspiration estimates shows a weak sensitivity to the choice of atmospheric forcing prescribed to the models, and the inter-model temporal inconsistencies are largest for high latitude inter-annual variations as well as for the inter-seasonal variations in the tropics. Evaluation of corresponding field-scale data also confirms the models' discrepancy for estimating evapotranspiration in high latitude regions. Analyses of sensitivity simulations that replace uncertain forcings (i.e. radiation, and precipitation) indicate that most models' evapotranspiration is slightly more sensitive to precipitation than to net radiation perturbations, and that the majority of the GSWP-2 models, at a global scale, are in a slightly moisture-limited evaporative condition.

In the context to faithfully quantify the global water budget, global water vapor variations from the SH07 study, as well as from the results of this study, indicate that variations of atmospheric storage are roughly 0.01% of global precipitation or evaporation. Thus, the scatter of the GSWP-2 evapotranspiration (2.5%) seems quite unsatisfactory. Rigorous error estimates in water vapor retrievals appear to remain elusive, yet more recent data from the AMSR-E and AIRS satellite instruments show great promise in providing a more comprehensive assessment in this regard. Nevertheless, the GSWP-2 results have clarified that improvements in model-based estimates will not be delivered through improvements in the atmospheric data used for inputs. Rather, refinements in the numerical recipes of these land models hold the most promise toward constraining our global water budgets.

This evaluation of the GSWP-2 modeled evapotranspiration places an emphasis to improve our estimates for high-latitude (cold-season) processes. We find only a small sample of data that currently exists to rectify this, and therefore future field experiments would need to augment the low density of data. Further, in these regions, many other processes are important for the controls on evapotranspiration that involve complex interactions with carbon cycling and the biogeochemistry of peatlands (Frolking *et al.*, 2008). At the time of the GSWP-2 exercise, none of the models employed had the capability to represent the dominant plant-type of peatlands: bryophytes (i.e. non-vascular plants with no roots or vascular systems). This may potentially be an additional key issue in the subsequent analyses and model development, as well as supporting field observations, to rectify the disparity seen in the GSWP-2 simulations, and for modeling evapotranspiration in general. Further, for these regions, which are dominated by cold-season processes, the modeling challenges of snow cover (Slater *et al.,* 2001) and seasonally frozen soil

(Luo *et al*., 2004) as well as their interplay with non-frozen soil hydro-thermal processes also contribute substantially to the evapotranspiration simulations. Thus, any subsequent field experiments will need to satisfy a multitude of observational requirements that span across many sub-disciplines of biogeophysical and biogeochemical processes.

Acknowledgements

The authors would like to thank Paul A. Dirmeyer and Taikan Oki for their invaluable contributions toward the planning and execution of the Global Soil Wetness Project Phase 2, without which this study would not be possible. In addition, the authors also wish to thank all the participants of GSWP-2 who contributed their time and resources to provide their model simulations, without which the fruits of GSWP-2 would have never been realized. The authors also wish to thank Andy Pitman for his valuable review and comments of an earlier version of this manuscript. This work was supported by the NASA Energy and Water-cycle Study (NEWS, grant #NNX06AC30A), under the NEWS Science and Integration Team activities.

5. REFERENCES

Ackerman, T. P., and G. M. Stokes, 2003: The Atmospheric Radiation Measurement Program. *Phys. Today*, 56, 38–44.

Adler, R. F., G. J. Huffman, A. Chang, R. Ferraro, P.-P. Xie, J. Janowiak, B. Rudolf, U. Schneider, S. Curtis, D. Bolvin, A. Gruber, J. Susskind, P. Arkin, and E. Nelkin, 2003: The Version-2 Global Precipitation Climatology Project (GPCP) monthly precipitation analysis. *J. Hydromet.*, 4, 1147-1167.

Baldocchi, D., and Coauthors, 2001: FLUXNET: A new tool to study the temporal and spatial variability of ecosystem-scale carbon dioxide, water vapor, and energy flux densities. *Bull. Amer. Meteor. Soc.*, 82, 2415–2434.

Bentamy, A., K. B. Katsaros, A. M Mestas-Nunez, W. M. Drennan, E. B. Forde, and H. Roquet, 2003: Satellite estimates of wind speed and latent heat flux over the global oceans. *J. Climate*, 16, 637-656.

Chen, T. H., A. Henderson-Sellers, P. C. D. Milly, A. J. Pitman, A. C. M. Beljaars, J. Polcher, F. Abramopoulos, A. Boone, S. Chang, F. Chen, Y. Dai, C. E. Desborough, R. E. Dickinson, L. Dumenil, M. Ek, J. R. Garratt, N. Gedney, Y. M. Gusev, J. Kim, R. Koster, E. A. Kowalczyk, K. Laval, J. Lean, D. Lettenmaier, X. Liang, J. F. Mahfouf, H. T. Mengelkamp, K. Mitchell, O. N. Nasonova, J. Noilhan, A. Robock, C. Rosenzweig, J. Schaake, C. A. Schlosser, J. P. Schulz, Y. Shao, A. B. Shmakin, D. L. Verseghy, P. Wetzel, E. F. Wood, Y. Xue, Z. L. Yang, and Q. Zeng, 1997: Cabauw experimental results from the project for intercomparison of land-surface parameterization schemes. *J.Clim.,* 10, 1194-1215.

Chou, S.-H., C.-L. Shie, B. Atlas, and J. Ardizzone, 2003: Surface turbulent heat and momentum fluxes over global oceans based on Goddard satellite retrievals, Version 2 (GSSTF2). *J. Climate*, 16, 3256-3273.

Cook, D. R., 2005: Energy Balance Bowen Ratio (EBBR) handbook. *ARM Tech. Rep. TR-037*, 23 pp.

Decharme, B., and H. Douville, 2006: Uncertainties in the GSWP-2 precipitation forcing and their impacts on regional and global hydrological simulations. *Climate Dyn.*, 27, 695-713.

Dirmeyer, P. A. and Tan, L., 2001: A multi-decadal global land-surface data set of state variables and fluxes. *COLA Tech. Rep. 102* [Available from the Center for Ocean-Land-Atmosphere Studies, 4041 Powder Mill Road, Suite 302, Calverton, MD 20705 USA], 43 pp.

Dirmeyer, P. A., Z. Guo, and X. Gao, 2004: Comparison, Validation, and Transferability of Eight Multiyear Global Soil Wetness Products, *J. Hydromet*, 5, 1011–1033.

Dirmeyer, P. A., X. Gao, M. Zhao, Z. Guo, T. Oki and N. Hanasaki , 2006: The Second Global Soil Wetness Project (GSWP-2): Multi-model analysis and implications for our perception of the land surface. *Bull. Amer. Meteor. Soc.*, 87,1381-1397.

Frolking, S., N. Roulet, and D. Lawrence, 2009: Issues related to incorporating northern peatlands into global climate models. AGU Monograph 'Northern Peatlands and Carbon Cycling' (in review).

Gao, X. and P. A. Dirmeyer, 2006: A multimodel analysis, validation, and transferability study of global soil wetness products. *J. Hydrometeor.*, 7, 1218-1236.

Guo, Z-C, P.A. Dirmeyer, X. Gao, and M. Zhao, 2007: Improving the quality of simulated soil moisture with a multi-model ensemble approach. *Q. J. R. Meteorol. Soc.*, 133: 731-747.

Hall, F. G., E. Brown de Colstoun, G. J. Collatz, D. Landis, P. Dirmeyer, A. Betts, G. Huffman, L. Bounoua and B. Meeson, 2006: ISLSCP Initiative II global data sets: Surface boundary conditions and atmospheric forcings for land-atmosphere studies. *J. Geophys. Res.*,111, doi:10.1029/2006JD007366.

Harmel, R.D., J. V. Bonta, and C. W. Richardson, 2007. The original USDA-ARS experimental watersheds in Texas and Ohio: Contributions from the past and visions for the future. *Trans. of the Amer. Soc. of Agr. and Bio. Eng.*, 50(5), 1669-1675.

International GEWEX Project Office, 2002: *The Second Golbal Soil Wetness Project Science and Implementation Plan*. IGPO Publication Series No. 37, 69 pp.

Kanamitsu, M., W. Ebisuzaki, J. Woollen, S.-K. Yang, J. J. Hnilo, M. Fiorino, and G. L. Potter, 2002: NCEP-DOE AMIP-II reanalysis (R-2). *Bull. Amer. Meteor. Soc.*, 83, 1631-1648.

Karam, H. N. and R. L. Bras, 2008: Climatological basin-scale Amazonian evapotranspiration estimated through a water budget analysis. *J. Hydromet.*, 9, 1048-1060.

Kumar, Sujay V., Rolf H. Reichle, Christa D. Peters-Lidard, Randal D. Koster, Xiwu Zhan, Wade T. Crow, John B. Eylander, and Paul R. Houser, 2008. A Land Surface Data Assimilation Framework using the Land Information System: Description and Applications, *Adv. Wat. Res.* (in press).

Loewe, F., 1957: Precipitation and evaporation in the Antarctic. *Met. Antarctic*, 11, 71-89.

Luo, L., A. Robock, K. Ya. Vinnikov, C. A. Schlosser, A. G. Slater, N. A. Speranskaya, and coauthors, 2004: Effects of frozen soil on soil temperature, spring infiltration, and runoff: Results from the PILPS 2(d) experiment at Valdai, Russia. *J. Hydromet,* 5, 334-351.

Rodell, M., J. S. Famiglietti, J. Chen, S. I. Seneviratne, P. Viterbo, S. Holl, and C. R. Wilson, 2004a: Basin scale estimates of evapotranspiration using GRACE and other observations. *Geophys. Res. Let.*, 31, L20504, doi:10.129/2004GL020873.

Rodell, M., P.R. Houser, U. Jambor, J. Gottschalck, K. Mitchell, C.-J. Meng, K. Arsenault, B. Cosgrove, J. Radakovich, M. Bosilovich, J.K. Entin, J.P. Walker, D. Lohmann, and D. Toll, 2004b: The Global Land Data Assimilation System, *BAMS*, 381-394.

Schlosser, C. A., and P. Houser, 2007: Assessing a satellite-era perspective of the global water cycle. *J. Climate*, 20, 1316-1338.

Slater, A. J., C. A. Schlosser, and co-authors, 2001: The representation of snow in land-surface schemes: Results from PILPS 2(d). *J. Hydromet*, 2, 7-25.

Song, J., M. L. Wesely, M. A. LeMone, R. L. Grossman, 2000: Estimating watershed evapotranspiration with PASS. Part II: Moisture budgets during drydown periods. *J. Hydromet.*, 1, 462-473.

Su, H., M. F. McCabe, E. F. Wood, Z. Su, and J. H. Prueger, 2005: Modeling evapotranspiration during SMACEX: Comparing two approaches for local- and regional-scale prediction. *J. Hydromet.*, 6, 910-922.

Swenson, S. and J. Wahr, 2006: Estimating large-scale precipitation minus evapotranspiration from GRACE satellite gravity measurements, *J. Hydromet.*, 7, 252-270.

Vonder Harr, T., and Co-Authors, 2003: Continuation of the NVAP global water vapor data sets for Pathfinder science analysis. *STC Technical Report 3333*. 44 pp. http://eosweb.larc.nasa.gov/ PRODOCS/nvap/sci_tech_report_3333.pdf

Walter, M. T., D. S. Wilks, J.-Y. Parlange, R. L. Schneider, 2004: Increasing evapotranspiration from the conterminous United States. *J. Hydromet.*, 5, 405-408.

Wang, K., Z. Li, M. Cribb, and M. Sparrow, 2007: A simple method to estimate actual evapotranspiration from a combination of net radiation, vegetation index, and temperature, *J. Geophys. Res.,* 112, D15107, doi:10.1029/2006JD008351.

Wang, K. and S. Liang, 2008: An improved method for estimating global evapotranspiration based on satellite determination of net radiation, vegetation index, temperature, and soil moisture, *J. Hydromet.*, 9, 712-727.

Werth, D. and R. Avissar, 2004: The regional evapotranspiration of the Amazon, *J. Hydromet.*, 5, 100-109.

Xie P. and P. A. Arkin, 1997: Global precipitation: A 17-year monthly analysis based on gauge observations, satellite estimates, and numerical model outputs. *Bull. Amer. Met. Soc.*, 78, 2539-2558.

Zhao, M., and P. Dirmeyer, 2003: Production and analysis of GSWP-2 near-surface meteorology data sets. *COLA Technical Report 159* [Available from the Center for Ocean-Land-Atmosphere Studies, 4041 Powder Mill Road, Suite 302, Calverton, MD 20705 USA], 22pp.

REPORT SERIES of the **MIT** *Joint Program on the Science and Policy of Global Change*

1. **Uncertainty in Climate Change Policy Analysis** *Jacoby & Prinn* December 1994
2. **Description and Validation of the MIT Version of the GISS 2D Model** *Sokolov & Stone* June 1995
3. **Responses of Primary Production and Carbon Storage to Changes in Climate and Atmospheric CO_2 Concentration** *Xiao et al.* October 1995
4. **Application of the Probabilistic Collocation Method for an Uncertainty Analysis** *Webster et al.* January 1996
5. **World Energy Consumption and CO_2 Emissions: 1950-2050** *Schmalensee et al.* April 1996
6. **The MIT Emission Prediction and Policy Analysis (EPPA) Model** *Yang et al.* May 1996 (*superseded by No. 125*)
7. **Integrated Global System Model for Climate Policy Analysis** *Prinn et al.* June 1996 (*superseded by No. 124*)
8. **Relative Roles of Changes in CO_2 and Climate to Equilibrium Responses of Net Primary Production and Carbon Storage** *Xiao et al.* June 1996
9. **CO_2 Emissions Limits:** ***Economic Adjustments and the Distribution of Burdens*** *Jacoby et al.* July 1997
10. **Modeling the Emissions of N_2O and CH_4 from the Terrestrial Biosphere to the Atmosphere** *Liu* Aug. 1996
11. **Global Warming Projections:** ***Sensitivity to Deep Ocean Mixing*** *Sokolov & Stone* September 1996
12. **Net Primary Production of Ecosystems in China and its Equilibrium Responses to Climate Changes** *Xiao et al.* November 1996
13. **Greenhouse Policy Architectures and Institutions** *Schmalensee* November 1996
14. **What Does Stabilizing Greenhouse Gas Concentrations Mean?** *Jacoby et al.* November 1996
15. **Economic Assessment of CO_2 Capture and Disposal** *Eckaus et al.* December 1996
16. **What Drives Deforestation in the Brazilian Amazon?** *Pfaff* December 1996
17. **A Flexible Climate Model For Use In Integrated Assessments** *Sokolov & Stone* March 1997
18. **Transient Climate Change and Potential Croplands of the World in the 21st Century** *Xiao et al.* May 1997
19. **Joint Implementation:** ***Lessons from Title IV's Voluntary Compliance Programs*** *Atkeson* June 1997
20. **Parameterization of Urban Subgrid Scale Processes in Global Atm. Chemistry Models** *Calbo* et al. July 1997
21. **Needed: A Realistic Strategy for Global Warming** *Jacoby, Prinn & Schmalensee* August 1997
22. **Same Science, Differing Policies;** ***The Saga of Global Climate Change*** *Skolnikoff* August 1997
23. **Uncertainty in the Oceanic Heat and Carbon Uptake and their Impact on Climate Projections** *Sokolov et al.* September 1997
24. **A Global Interactive Chemistry and Climate Model** *Wang, Prinn & Sokolov* September 1997
25. **Interactions Among Emissions, Atmospheric Chemistry & Climate Change** *Wang & Prinn* Sept. 1997
26. **Necessary Conditions for Stabilization Agreements** *Yang & Jacoby* October 1997
27. **Annex I Differentiation Proposals:** ***Implications for Welfare, Equity and Policy*** *Reiner & Jacoby* Oct. 1997
28. **Transient Climate Change and Net Ecosystem Production of the Terrestrial Biosphere** *Xiao et al.* November 1997
29. **Analysis of CO_2 Emissions from Fossil Fuel in Korea: 1961–1994** *Choi* November 1997
30. **Uncertainty in Future Carbon Emissions:** ***A Preliminary Exploration*** *Webster* November 1997
31. **Beyond Emissions Paths:** ***Rethinking the Climate Impacts of Emissions Protocols*** *Webster & Reiner* November 1997
32. **Kyoto's Unfinished Business** *Jacoby et al.* June 1998
33. **Economic Development and the Structure of the Demand for Commercial Energy** *Judson et al.* April 1998
34. **Combined Effects of Anthropogenic Emissions and Resultant Climatic Changes on Atmospheric OH** *Wang & Prinn* April 1998
35. **Impact of Emissions, Chemistry, and Climate on Atmospheric Carbon Monoxide** *Wang & Prinn* April 1998
36. **Integrated Global System Model for Climate Policy Assessment:** ***Feedbacks and Sensitivity Studies*** *Prinn et al.* June 1998
37. **Quantifying the Uncertainty in Climate Predictions** *Webster & Sokolov* July 1998
38. **Sequential Climate Decisions Under Uncertainty:** ***An Integrated Framework*** *Valverde et al.* September 1998
39. **Uncertainty in Atmospheric CO_2 (Ocean Carbon Cycle Model Analysis)** *Holian* Oct. 1998 (*superseded by No. 80*)
40. **Analysis of Post-Kyoto CO_2 Emissions Trading Using Marginal Abatement Curves** *Ellerman & Decaux* Oct. 1998
41. **The Effects on Developing Countries of the Kyoto Protocol and CO_2 Emissions Trading** *Ellerman et al.* November 1998
42. **Obstacles to Global CO_2 Trading:** ***A Familiar Problem*** *Ellerman* November 1998
43. **The Uses and Misuses of Technology Development as a Component of Climate Policy** *Jacoby* November 1998
44. **Primary Aluminum Production:** ***Climate Policy, Emissions and Costs*** *Harnisch et al.* December 1998
45. **Multi-Gas Assessment of the Kyoto Protocol** *Reilly et al.* January 1999
46. **From Science to Policy:** ***The Science-Related Politics of Climate Change Policy in the U.S.*** *Skolnikoff* January 1999
47. **Constraining Uncertainties in Climate Models Using Climate Change Detection Techniques** *Forest et al.* April 1999
48. **Adjusting to Policy Expectations in Climate Change Modeling** *Shackley et al.* May 1999
49. **Toward a Useful Architecture for Climate Change Negotiations** *Jacoby et al.* May 1999
50. **A Study of the Effects of Natural Fertility, Weather and Productive Inputs in Chinese Agriculture** *Eckaus & Tso* July 1999
51. **Japanese Nuclear Power and the Kyoto Agreement** *Babiker, Reilly & Ellerman* August 1999
52. **Interactive Chemistry and Climate Models in Global Change Studies** *Wang & Prinn* September 1999
53. **Developing Country Effects of Kyoto-Type Emissions Restrictions** *Babiker & Jacoby* October 1999

Contact the Joint Program Office to request a copy. The Report Series is distributed at no charge.

Contact the Joint Program Office to request a copy. The Report Series is distributed at no charge.

105. Analysis of Strategies of Companies under Carbon Constraint *Hashimoto* January 2004
106. Climate Prediction: ***The Limits of Ocean Models*** *Stone* February 2004
107. Informing Climate Policy Given Incommensurable Benefits Estimates *Jacoby* February 2004
108. Methane Fluxes Between Terrestrial Ecosystems and the Atmosphere at High Latitudes During the Past Century *Zhuang et al.* March 2004
109. Sensitivity of Climate to Diapycnal Diffusivity in the Ocean *Dalan et al.* May 2004
110. Stabilization and Global Climate Policy *Sarofim et al.* July 2004
111. Technology and Technical Change in the MIT EPPA Model *Jacoby et al.* July 2004
112. The Cost of Kyoto Protocol Targets: ***The Case of Japan*** *Paltsev et al.* July 2004
113. Economic Benefits of Air Pollution Regulation in the USA: ***An Integrated Approach*** *Yang et al.* (revised) Jan. 2005
114. The Role of Non-CO_2 Greenhouse Gases in Climate Policy: ***Analysis Using the MIT IGSM*** *Reilly et al.* Aug. '04
115. Future U.S. Energy Security Concerns *Deutch* Sep. '04
116. Explaining Long-Run Changes in the Energy Intensity of the U.S. Economy *Sue Wing* Sept. 2004
117. Modeling the Transport Sector: ***The Role of Existing Fuel Taxes in Climate Policy*** *Paltsev et al.* November 2004
118. Effects of Air Pollution Control on Climate *Prinn et al.* January 2005
119. Does Model Sensitivity to Changes in CO_2 Provide a Measure of Sensitivity to the Forcing of Different Nature? *Sokolov* March 2005
120. What Should the Government Do To Encourage Technical Change in the Energy Sector? *Deutch* May '05
121. Climate Change Taxes and Energy Efficiency in Japan *Kasahara et al.* May 2005
122. A 3D Ocean-Seaice-Carbon Cycle Model and its Coupling to a 2D Atmospheric Model: ***Uses in Climate Change Studies*** *Dutkiewicz et al.* (revised) November 2005
123. Simulating the Spatial Distribution of Population and Emissions to 2100 *Asadoorian* May 2005
124. MIT Integrated Global System Model (IGSM) Version 2: ***Model Description and Baseline Evaluation*** *Sokolov et al.* July 2005
125. The MIT Emissions Prediction and Policy Analysis (EPPA) Model: ***Version 4*** *Paltsev et al.* August 2005
126. Estimated PDFs of Climate System Properties Including Natural and Anthropogenic Forcings *Forest et al.* September 2005
127. An Analysis of the European Emission Trading Scheme *Reilly & Paltsev* October 2005
128. Evaluating the Use of Ocean Models of Different Complexity in Climate Change Studies *Sokolov et al.* November 2005
129. *Future* Carbon Regulations and *Current* Investments in Alternative Coal-Fired Power Plant Designs *Sekar et al.* December 2005
130. Absolute vs. Intensity Limits for CO_2 Emission Control: ***Performance Under Uncertainty*** *Sue Wing et al.* January 2006
131. The Economic Impacts of Climate Change: ***Evidence from Agricultural Profits and Random Fluctuations in Weather*** *Deschenes & Greenstone* January 2006
132. The Value of Emissions Trading *Webster et al.* Feb. 2006
133. Estimating Probability Distributions from Complex Models with Bifurcations: ***The Case of Ocean Circulation Collapse*** *Webster et al.* March 2006
134. Directed Technical Change and Climate Policy *Otto et al.* April 2006
135. Modeling Climate Feedbacks to Energy Demand: ***The Case of China*** *Asadoorian et al.* June 2006
136. Bringing Transportation into a Cap-and-Trade Regime *Ellerman, Jacoby & Zimmerman* June 2006
137. Unemployment Effects of Climate Policy *Babiker & Eckaus* July 2006
138. Energy Conservation in the United States: ***Understanding its Role in Climate Policy*** *Metcalf* Aug. '06
139. Directed Technical Change and the Adoption of CO_2 Abatement Technology: ***The Case of CO_2 Capture and Storage*** *Otto & Reilly* August 2006
140. The Allocation of European Union Allowances: ***Lessons, Unifying Themes and General Principles*** *Buchner et al.* October 2006
141. Over-Allocation or Abatement? ***A preliminary analysis of the EU ETS based on the 2006 emissions data*** *Ellerman & Buchner* December 2006
142. Federal Tax Policy Towards Energy *Metcalf* Jan. 2007
143. Technical Change, Investment and Energy Intensity *Kratena* March 2007
144. Heavier Crude, Changing Demand for Petroleum Fuels, Regional Climate Policy, and the Location of Upgrading Capacity *Reilly et al.* April 2007
145. Biomass Energy and Competition for Land *Reilly & Paltsev* April 2007
146. Assessment of U.S. Cap-and-Trade Proposals *Paltsev et al.* April 2007
147. A Global Land System Framework for Integrated Climate-Change Assessments *Schlosser et al.* May 2007
148. Relative Roles of Climate Sensitivity and Forcing in Defining the Ocean Circulation Response to Climate Change *Scott et al.* May 2007
149. Global Economic Effects of Changes in Crops, Pasture, and Forests due to Changing Climate, CO_2 and Ozone *Reilly et al.* May 2007
150. U.S. GHG Cap-and-Trade Proposals: ***Application of a Forward-Looking Computable General Equilibrium Model*** *Gurgel et al.* June 2007
151. Consequences of Considering Carbon/Nitrogen Interactions on the Feedbacks between Climate and the Terrestrial Carbon Cycle *Sokolov et al.* June 2007
152. Energy Scenarios for East Asia: 2005-2025 *Paltsev & Reilly* July 2007
153. Climate Change, Mortality, and Adaptation: ***Evidence from Annual Fluctuations in Weather in the U.S.*** *Deschênes & Greenstone* August 2007

Contact the Joint Program Office to request a copy. The Report Series is distributed at no charge.

154. Modeling the Prospects for Hydrogen Powered Transportation Through 2100 *Sandoval et al.* February 2008
155. Potential Land Use Implications of a Global Biofuels Industry *Gurgel et al.* March 2008
156. Estimating the Economic Cost of Sea-Level Rise *Sugiyama et al.* April 2008
157. Constraining Climate Model Parameters from Observed 20th Century Changes *Forest et al.* April 2008
158. Analysis of the Coal Sector under Carbon Constraints *McFarland et al.* April 2008
159. Impact of Sulfur and Carbonaceous Emissions from International Shipping on Aerosol Distributions and Direct Radiative Forcing *Wang & Kim* April 2008
160. Analysis of U.S. Greenhouse Gas Tax Proposals *Metcalf et al.* April 2008
161. A Forward Looking Version of the MIT Emissions Prediction and Policy Analysis (EPPA) Model *Babiker et al.* May 2008
162. The European Carbon Market in Action: *Lessons from the first trading period* Interim Report *Convery, Ellerman, & de Perthuis* June 2008
163. The Influence on Climate Change of Differing Scenarios for Future Development Analyzed Using the MIT Integrated Global System Model *Prinn et al.* September 2008
164. Marginal Abatement Costs and Marginal Welfare Costs for Greenhouse Gas Emissions Reductions: *Results from the EPPA Model* *Holak et al.* November 2008
165. Uncertainty in Greenhouse Emissions and Costs of Atmospheric Stabilization *Webster et al.* November 2008
166. Sensitivity of Climate Change Projections to Uncertainties in the Estimates of Observed Changes in Deep-Ocean Heat Content *Sokolov et al.* November 2008
167. Sharing the Burden of GHG Reductions *Jacoby et al.* November 2008
168. Unintended Environmental Consequences of a Global Biofuels Program *Melillo et al.* January 2009
169. Probabilistic Forecast for 21st Century Climate Based on Uncertainties in Emissions (without Policy) and Climate Parameters *Sokolov et al.* January 2009
170. The EU's Emissions Trading Scheme: *A Proto-type Global System?* *Ellerman* February 2009
171. Designing a U.S. Market for CO_2 *Parsons et al.* February 2009
172. Prospects for Plug-in Hybrid Electric Vehicles in the United States & Japan: *A General Equilibrium Analysis* *Karplus et al.* April 2009
173. The Cost of Climate Policy in the United States *Paltsev et al.* April 2009
174. A Semi-Empirical Representation of the Temporal Variation of Total Greenhouse Gas Levels Expressed as Equivalent Levels of Carbon Dioxide *Huang et al.* June 2009
175. Potential Climatic Impacts and Reliability of Very Large Scale Wind Farms *Wang & Prinn* June 2009
176. Biofuels, Climate Policy and the European Vehicle Fleet *Gitiaux et al.* August 2009
177. Global Health and Economic Impacts of Future Ozone Pollution *Selin et al.* August 2009
178. Measuring Welfare Loss Caused by Air Pollution in Europe: *A CGE Analysis* *Nam et al.* August 2009
179. Assessing Evapotranspiration Estimates from the Global Soil Wetness Project Phase 2 (GSWP-2) Simulations *Schlosser and Gao* September 2009

Contact the Joint Program Office to request a copy. The Report Series is distributed at no charge.